Supplementary data for

Structural basis of the PE–PPE protein interaction in *Mycobacterium tuberculosis*

Xin Chen[1], Hiu-fu Cheng[1], Junwei Zhou[1], Chiu-yeung Chan[2], Kwok-fai Lau[1], Stephen Kwok-wing Tsui[3] and Shannon Wing-ngor Au[1#]

[1] Centre for Protein Science and Crystallography, School of Life Sciences, The Chinese University of Hong Kong, Hong Kong, China

[2] Department of Microbiology, The Chinese University of Hong Kong, Hong Kong, China

[3] School of Biomedical Sciences, The Chinese University of Hong Kong, Hong Kong, China

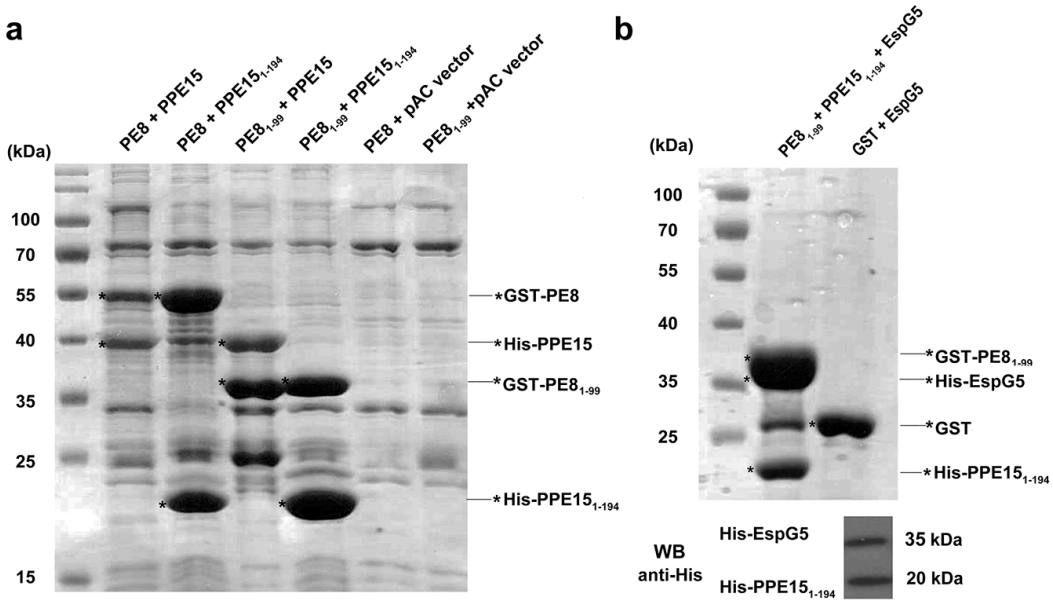

Figure S1. Interaction studies of EspG5–PE8–PPE15 by pull-down assays. (a) Mapping of the minimum regions required for PE8–PPE15 interaction. Fragments of PE8 containing residues 1-99, and of PPE15 containing residues 1-194 were constructed based on the solved PE25–PPE41 structure, the secondary structure prediction of PE8–PPE15 and limited proteolysis combined with mass spectrometry. After co-expression, clear lysate was subjected to nickel pull-down. Individually expressed GST-PE8 and -PE8$_{1-99}$ were used as negative control. The results show that PE8$_{1-99}$ and PPE15$_{1-194}$ fragments are the minimal regions for molecular interaction. (b) Interaction of EspG5 and PE–PPE studied by GST-pull down assay. Lysates containing GST-PE8$_{1-99}$/His-PPE15$_{1-194}$ and His-EspG5 were incubated and subjected to pull down assay using glutathioine sepharose. GST protein alone was used as negative control. GST-PE8$_{1-99}$ and His-EspG5 are of similar molecular size and co-migrated in SDS-PAGE. The existences of His-EspG5 and His-PPE15$_{1-194}$ after pull-down assays were confirmed by immunoblotting with anti-His antibody.

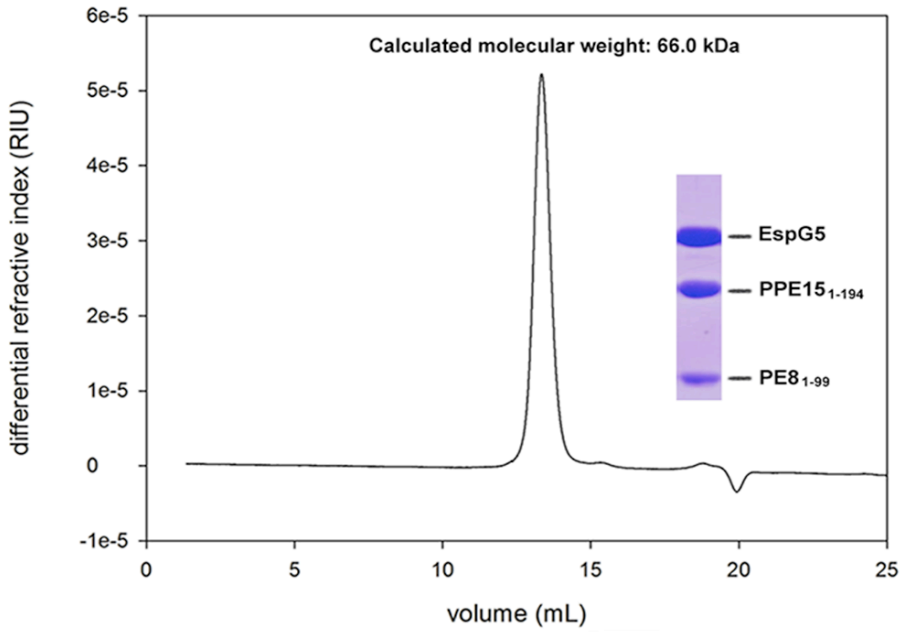

Figure S2. Molecular mass determination by static light scattering analysis. Purified EspG5–$PE8_{1\text{-}99}$–$PPE15_{1\text{-}194}$ complex was analyzed by static light scattering in combination with Superdex 200 size exclusion chromatography. The molecular weight was calculated to be 66.0 kDa, suggesting that EspG5–$PE8_{1\text{-}99}$–$PPE15_{1\text{-}194}$ complex is in a stoichiometry ratio of 1:1:1. Protein samples taken from the elution peak were validated by SDS-PAGE.

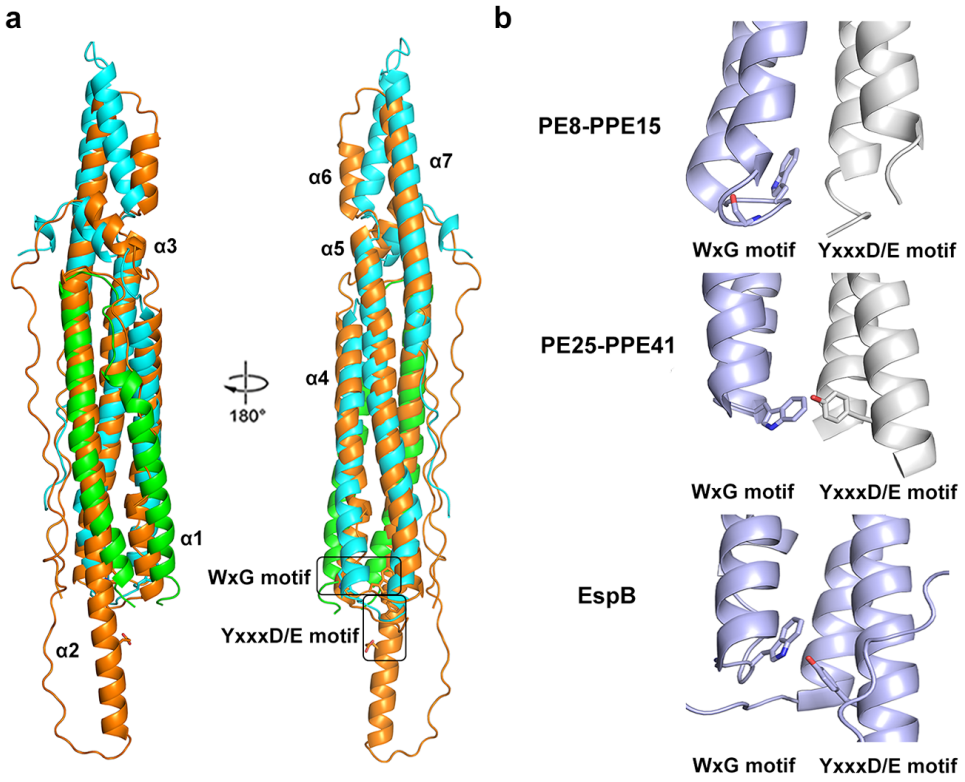

Figure S3. Structural comparison of the PE8–PPE15, PE25–PPE41 and EspB proteins. (a) Superimposition of PE8$_{1\text{-}99}$–PPE15$_{1\text{-}194}$ (green and cyan) and EspB (orange), showing similar overall fold. Helices α1-α7 of EspB are indicated. (b) Different conformations of YxxxD/E and WxG motifs in PE8–PPE15, PE25–PPE41 and EspB structures.

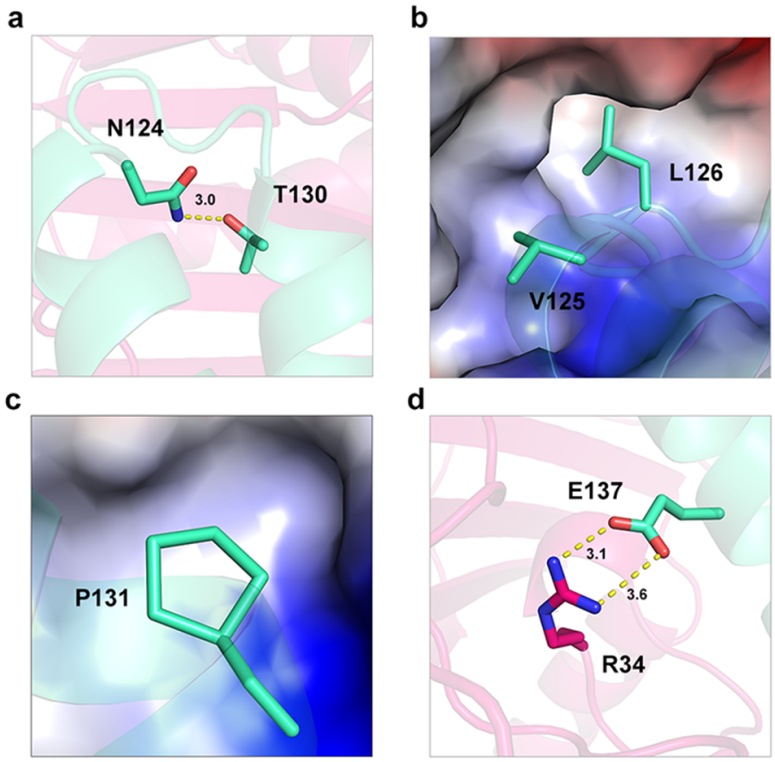

Figure S4. Binding interface of EspG5 and PPE15. (a) Stability of the loop between helix α4 and helix α5 of PPE15 is stabilized by a hydrogen bond between Thr130 and Asn124. (b, c) Hydrophobic contacts between EspG5 and PPE15. Val125 and Leu126 at the α4-α5 loop, and Pro131 at helix α5 of PPE15 are represented by stick mode and colored in cyan. EspG5 is shown as molecular surface. (d) Salt bridge between Glu137 in PPE15 and Arg34 in EspG5.

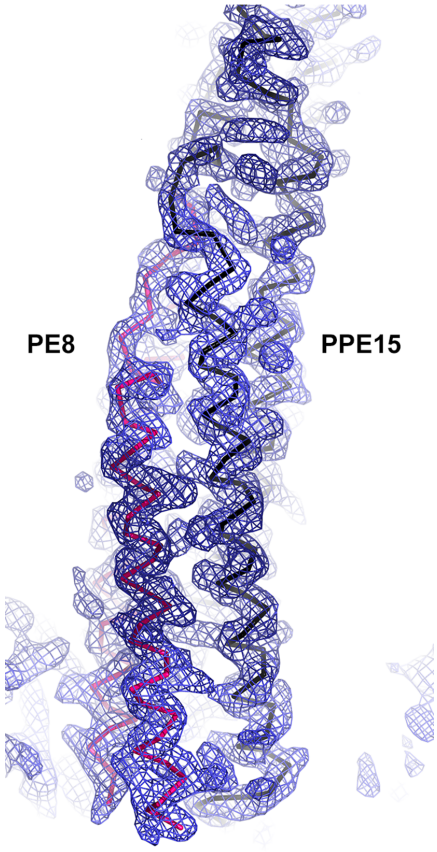

Figure S5. Electron density map for PE8$_{1-99}$ and PPE15$_{1-194}$. 2Fo-Fc map at 2.9-Å resolution (contour level of 1) was presented. Helices of PE8$_{1-99}$ and PPE15$_{1-194}$ are presented as ribbon and colored in red and black, respectively.

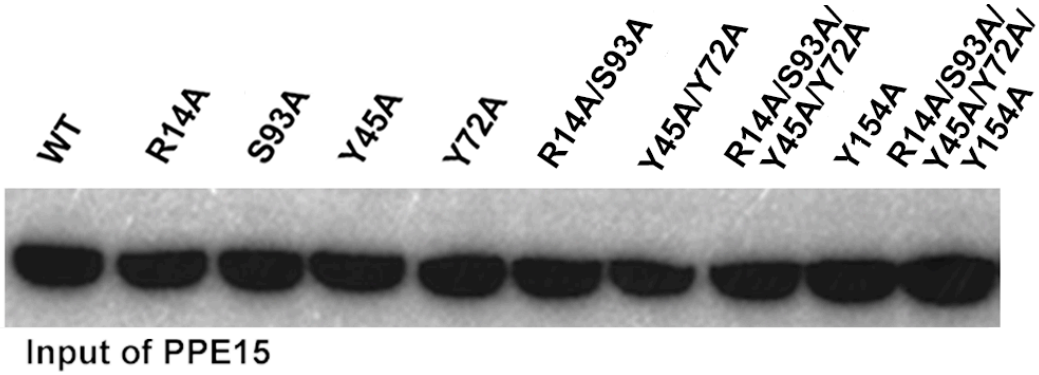

Figure S6. Expression and solubility of PPE15 wild type and mutants. GST-tagged $PE8_{1-99}$ and His-tagged PPE15 were co-expressed. His-tagged PPE15 in the soluble fractions were detected by Western blotting using anti-His antibody. The results show that the expression level and solubility of PPE15 mutants are similar with that of the wild type (WT).

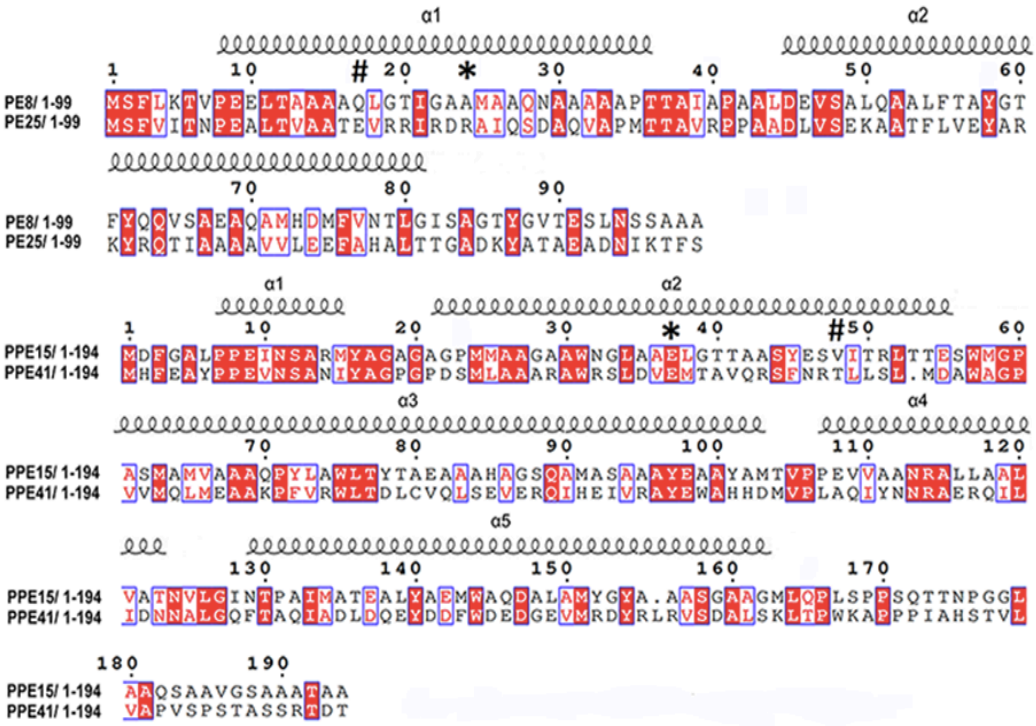

Figure S7. Structure-based sequence alignments of PE8 (residues from 1 to 99) with PE25, and PPE15 (residues from 1 to 194) with PPE41. The secondary structure elements of PE8 and PPE15 are shown above the protein sequence. Residues involve in salt bridge (PE25/Arg24 and PPE41/Glu37) and hydrogen bond formation (PE25/Glu17 and PPE41/Thr48) are indicated by * and #, respectively. The conserved hydrogen bond formed between PE25/Ser48 and PPE41/Tyr154 is not indicated.

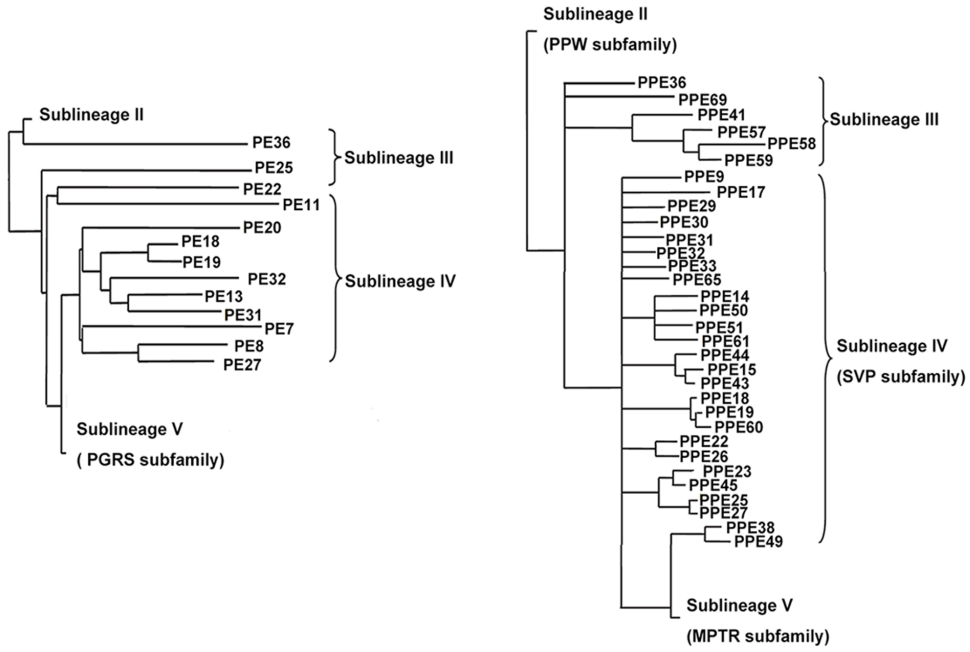

Figure S8. Phylogenetic tree of PE and PPE proteins. PE and PPE proteins in sublineage III and IV are listed. PE27–PPE43, PE13–PPE18 and PE32–PPE65 are all classified in sublineage IV. The close phylogenetic relationships between PE8 and PE27, and PPE15 and PPE43 suggest that they are co-evoluted and co-expanded.

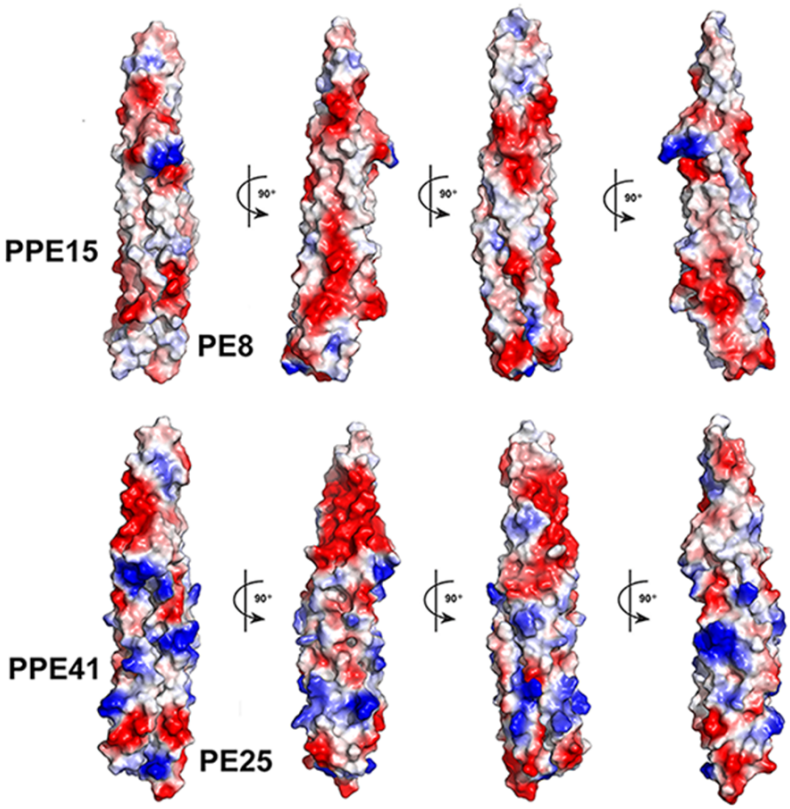

Figure S9. Electrostatic surface of $PE8_{1\text{-}99}$–$PPE15_{1\text{-}194}$ (top) and PE25–PPE41 (bottom) showing distinct molecular surface and charge distribution.

Table S1 Identification of PE8 and PPE15 homologues based on the sequence alignment of PE (residues 1-99) and PPE (residues 1-194) domains

Homologs of PE8	PE13 (59%), PE16 (49%), PE18 (62%), PE19 (64%), PE27 (73%), PE31 (49%), PE32 (49%), PE_PGRS 22 (56%)
Homologs of PPE15	PPE6 (51%), PPE8 (54%), PPE9 (61%), PPE10 (54%), PPE12 (51%), PPE13 (55%), PPE14 (58%), PPE16 (53%), PPE18 (55%), PPE21 (54%), PPE24 (51%), PPE28 (54%), PPE29 (60%), PPE32 (64%), PPE34 (50%), PPE40 (54%), PPE42 (56%), PPE43 (82%), PPE44 (69%), PPE50 (54%), PPE52 (64%), PPE53 (54%), PPE54 (53%), PPE55 (52%), PPE56 (55%), PPE62 (53%), PPE63 (55%), PPE64 (55%), PPE65 (64%)

Brackets indicate the percentage of sequence identities with PE8 or PPE15.